# Laser processing of polymer nanocomposite thin films

A. T. Sellinger, E. M. Leveugle, K. Gogick, L. V. Zhigilei, and J. M. Fitz-Gerald[a)]
*Department of Materials Science and Engineering, University of Virginia, 116 Engineers Way, Charlottesville, Virginia 22904*

(Received 4 October 2005; accepted 26 December 2005; published 23 June 2006)

Current biotechnology and sensor research has enhanced the drive to establish viable methods for depositing high-quality polymer thin films. In this research, thin films of poly(methyl methacrylate) (PMMA) were prepared by matrix-assisted pulsed-laser evaporation (MAPLE). Up to 2 wt % of carbon nanotubes were subsequently added to MAPLE target systems for deposition of polymer nanocomposite films. Targets were ablated using a 248 nm (KrF) laser at fluences ranging from 0.045 to 0.75 J/cm$^2$. In addition, polymer concentration in MAPLE targets was varied between 1 and 5 wt % relative to the matrix solvent, in this case toluene. Films were deposited on Si substrates at room temperature in an Ar atmosphere. Molecular-dynamics simulations of MAPLE were utilized for interpretation of experimental observations. Particularly, the ejection of large clusters consisting of both PMMA and toluene molecules was studied and related to the observed morphology of the deposited films. © *2006 American Vacuum Society.* [DOI: 10.1116/1.2167980]

## I. INTRODUCTION

Matrix-assisted pulsed-laser evaporation (MAPLE) was originally developed as a "gentle" alternative to conventional pulsed-laser deposition (PLD) of organic molecules.[1] Since its conception, MAPLE has been utilized for depositing a wide range of organic materials, including polymers,[2–4] polymer nanocomposites,[5] and chemoselective polymers.[1]

Carbon-nanotube-reinforced polymer thin-film growth is currently a thriving field of research due to the useful properties that nanocomposite thin films tend to exhibit.[6–12] Polymer thin films infused with carbon nanotubes (CNTs) often display enhancements in properties such as light emission, mechanical moduli, and electrical conductivity over the polymer matrix alone.[6–8] The levels at which these enhanced films perform is directly related to the arrangement of individual CNTs relative to one another. The tendency of CNTs to agglomerate makes uniform CNT dispersion and orientation throughout a polymer matrix difficult using conventional deposition techniques. The laser-assisted approach to polymer-CNT thin-film growth could provide an attractive alternative to conventional thin-film fabrication processes.

The work presented in this article studies the effects laser fluence and target polymer loading have on polymer thin-film formation during MAPLE as an initial step in the development of polymer nanocomposite thin films. Coarse-grained molecular-dynamics simulations are performed in parallel with experiments, assisting in the interpretation of the morphological features observed in the deposited films.

## II. EXPERIMENTAL AND COMPUTATIONAL SETUPS

Targets of poly(methyl methacrylate) (PMMA, $M_w = 15\,000$) dissolved in toluene were prepared with polymer concentrations of 1, 3, or 5 wt % by ultrasonication and flash freezing in liquid nitrogen for 300 s ($T_{\text{melt}}$ toluene ~178 K). Toluene was selected as the matrix solvent due to both its high absorption in the UV and its dissolution characteristics. Depositions were performed onto *p*-type, single-crystal Si substrates at a distance of 7 cm from the target. The chamber was initially pumped down to a base pressure of $2 \times 10^{-5}$ Torr prior to the deposition. By throttling the vacuum systems during deposition, the pressure was stabilized at 100 mTorr while maintaining a continuous Ar flow of 3 SCCM (standard cubic centimeter per minute). The laser fluence was varied from 0.045 to 0.75 J/cm$^2$ using a pulsed excimer laser [$\lambda = 248$ nm, 25 ns full width at half maximum (FWHM)] operating at a frequency of 5 Hz. To minimize target surface effects, dynamic rastering of the beam was performed. The surface characteristics of the deposited films were characterized using a JEOL 6700 scanning electron microscope (SEM).

A coarse-grained molecular-dynamics model combining the "breathing sphere" model[13,14] for representation of matrix molecules and the "bead-and-spring" model[15] for polymer molecules was utilized in MAPLE simulations. A computational cell with dimensions of $40 \times 40 \times 60$ nm (~650 000 molecules) was used in the simulations, with the polymer chains randomly and uniformly distributed throughout the sample. Each chain contained 100 monomer units, with each unit being of the same molecular weight as a single-matrix molecule, 100 Da. This number corresponds to the actual weight of a PMMA monomer and is close to the actual weight of a toluene molecule, 92 Da. The simulations were performed for a range of laser fluences and PMMA concentrations of 1, 3, and 6 wt %.

A 50 ps laser-pulse duration and 50 nm penetration depth were used in the simulations to reproduce the experimental regime of thermal confinement. The condition for the thermal confinement of the deposited laser energy can be expressed as $\tau_p < \tau_{\text{th}} = \{L_p^2\}/\{AD_T\}$, where $D_T$ is the thermal diffusivity of the irradiated material, $L_p$ is the laser penetra-

a)Electronic mail: jmf8h@virginia.edu and jmf8h@unix.mail.virginia.edu

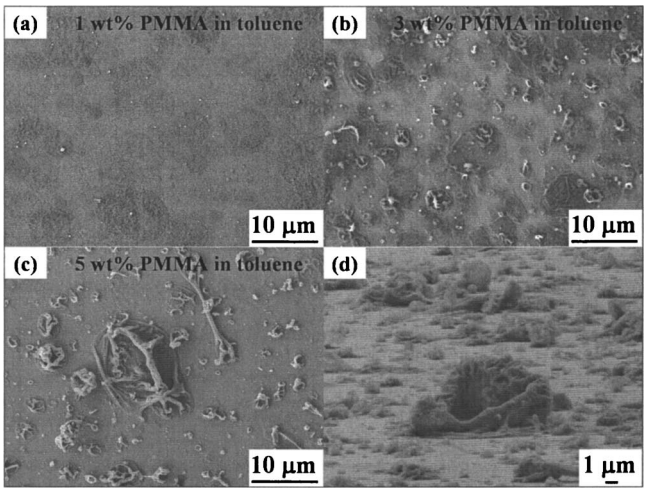


FIG. 1. SEM micrographs of PMMA films deposited at a laser fluence of ≈0.45 J/cm$^2$ and a PMMA concentration of (a) 1 wt % PMMA, (b) 3 wt % PMMA, and (c) 5 wt % PMMA. (d) SEM micrograph of the PMMA film pictured in (c) tilted 85° from the surface normal. As PMMA concentration was increased, the mean size and number of surface features also increased.

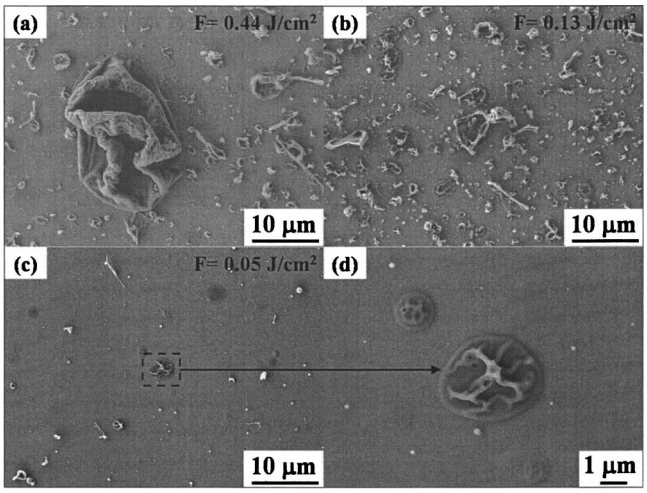


FIG. 2. SEM micrographs of PMMA films deposited using a PMMA concentration of 5 wt % and laser fluences of (a) 0.44, (b) 0.13, and (c) 0.05 J/cm$^2$. (d) SEM micrograph of a surface feature present on the PMMA film pictured in (c) at higher magnification. As laser fluence was increased from 0.05 to 0.10 J/cm$^2$, the number density of surface features also increased. As laser fluence was increased above 0.10 J/cm$^2$, the effect of fluence on particle number density was less pronounced, as an abrupt increase in material ejection was observed.

tion depth or the size of the absorbing structure, and $A$ is a constant defined by the geometry of the absorbing region.[14] The pulse duration of 50 ps is short relative to the characteristic thermal diffusion time across the absorption depth, $\tau_{th} \approx 250$ ps, but longer than the mechanical equilibration time of the absorbing volume, $\tau_s \approx L_p/C_s \approx 38$ ps, where $C_s$ is the speed of sound in the irradiated material. Therefore, these simulations are in the regime of thermal confinement, but not in the regime of thermoelastic stress confinement. Similarly, for experiments, $\tau_{th}$ and $\tau_s$ can be estimated to be $\approx 90$ $\mu$s and 3 ns, respectively, also placing experimental conditions in the thermal confinement regime.

In the thermal confinement regime, heat conduction does not contribute to the energy redistribution during the laser pulse and the thermal energy is largely confined within the absorbing region. Moreover, the pulse duration in the regime of thermal confinement is usually shorter than the time needed for the formation and diffusion of a gas-phase bubble in the process of heterogeneous boiling.[16] As a result, the absorbing material can be overheated far beyond the boiling temperature, turning a normal surface evaporation at low laser fluences into an explosive vaporization, or phase explosion, at higher fluences.[14,17]

## III. RESULTS AND DISCUSSION

Laser fluence and polymer loading in the target were found to have significant effects on the surface morphology of PMMA films, as previously shown for other MAPLE and PLD systems.[3] The size and number of surface features tended to increase with increasing PMMA concentration. Figures 1(a)–1(d) show representative SEM images displaying a film-morphology dependence on PMMA concentration for three films deposited at a fluence of ≈0.45 J/cm$^2$. As PMMA concentration increases from [Fig. 1(a)] 1 wt % to [Fig. 1(c)] 5 wt %, the mean number and size of surface features also increase. Figure 1(d) is a tilted SEM micrograph of one of the larger surface features present on the film pictured in Fig. 1(c). The feature's deflated appearance was characteristic of many of the surface particles observed. Similar MAPLE-induced morphological characteristics were observed in other polymer systems using chloroform as the matrix solvent.[3] Ideally, the toluene molecules are vaporized from the target and immediately pumped out of the chamber. However, it has been hypothesized that for this polymer-solvent system, clusters of material comprised of both toluene and PMMA are ejected from the target. Whether the clusters still contain toluene molecules upon deposition onto the substrate is still under investigation.

Figures 2(a)–2(d) show SEM micrographs of films deposited at three different fluences while holding the PMMA concentration constant at 5 wt % relative to the solvent. For fluences below 0.10 J/cm$^2$, the number density of the surface features increases with laser fluence. For fluences exceeding 0.10 J/cm$^2$, however, the effect of fluence on particle number density is much less pronounced, as a sharp rise in material ejection was observed. The film in Fig. 2(c) was formed close to the ablation threshold for this system, which may explain the sudden increase in material removal from the target once the fluence reached a critical value. Figure 2(d) is a SEM micrograph showing a close up of one of the surface features from the film pictured in Fig. 2(c). Even at a fluence of 0.045 J/cm$^2$, significant clusters of material were ablated from the target. Incidentally, the association of the ejection of large clusters with the ablation threshold is supported by molecular-dynamics simulations, where a sharp threshold for ablation and the ejection of a small number of large particles were observed.

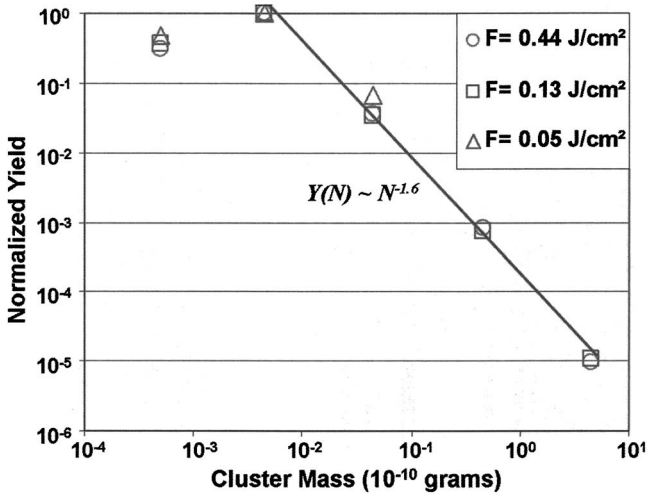


FIG. 3. Plot of normalized particle yield as a function of particle mass for the three films pictured in Fig. 2. A power-law dependence was observed for larger surface clusters, where $N$ represents the cluster mass.

The plot pictured in Fig. 3 shows the normalized yield of deposited particles as a function of cluster mass for the films pictured in Fig. 2. The plot was generated from representative 0.01 $mm^2$ areas of each film. The areas of surface features were measured and subsequently converted to volumes using a conversion factor that was determined through careful examination of tilted high-resolution SEM images of representative surface features. The conversion factor was determined as a function of cluster size. Cluster masses were subsequently calculated using a density value for PMMA provided by the manufacturer. The mass-distribution trends for the three fluences in question are similar, suggesting that the mass distribution of deposited clusters has a limited dependence on laser fluence. The mass distribution for large clusters can be described by a power-law dependence, $Y(N) \sim N^{-t}$, where $N$ represents the cluster mass and $t \approx 1.6$. A similar power-law dependence with $t \approx 1.3$ was reported for size distributions of high-mass clusters in molecular-dynamics simulations of laser ablation of molecular targets.[17]

The results of molecular-dynamics simulations of MAPLE provided insight into the origin of the observed film morphology. In the simulations, at all fluences exceeding the ablation threshold the polymer molecules were found to be ejected only as parts of matrix-polymer droplets/clusters. For the same polymer concentration, a higher fluence yielded more clusters with a broader range of sizes. Figure 4 provides a visual picture of the formation of a matrix-polymer cluster containing five polymer chains, as observed in a simulation performed for a target containing 3 wt % PMMA irradiated by a 50 ps laser pulse at a fluence of 8 $mJ/cm^2$. A series of snapshots shows the evolution of the cluster from 400 ps after separation from the target to the time when the cluster acquires an equilibrium spherical geometry 600 ps later. The diameter of the cluster at 1 ns is on the order of 10 nm, which is much smaller than many of the clusters produced experimentally, as observed via SEM. The maximum size of clusters ejected in the simulations is limited by

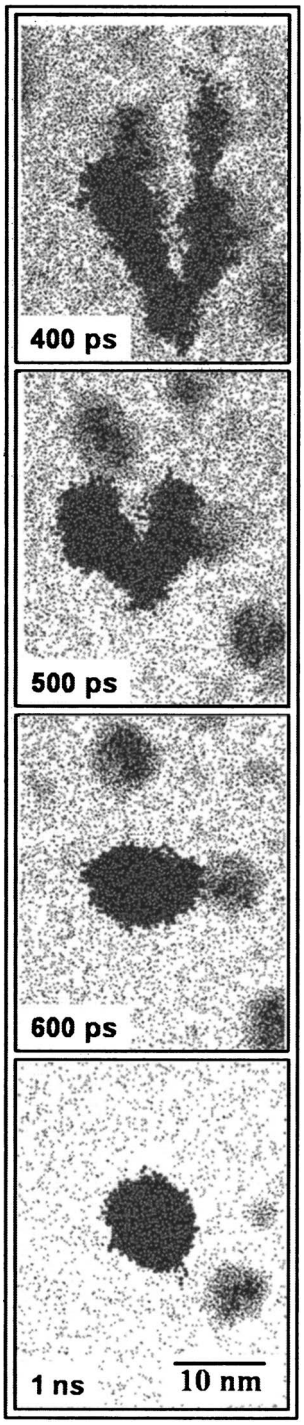


FIG. 4. Snapshots from the ablation plume generated in a molecular-dynamics simulation of laser ablation of a MAPLE target with 3 wt % polymer concentration. The evolution of a representative matrix-polymer cluster is shown at different times after ejection from the target.

the size of the ablation volume, which, in turn, is typically comparable to the laser penetration depth. With laser penetration depths on the order of 50 nm in simulations and 4 $\mu$m in experiments, the simulations can be considered scaled-down versions of experiments. Therefore, the behavior of the cluster illustrated in Fig. 4 can be taken to be representative of the behavior of much larger clusters ejected

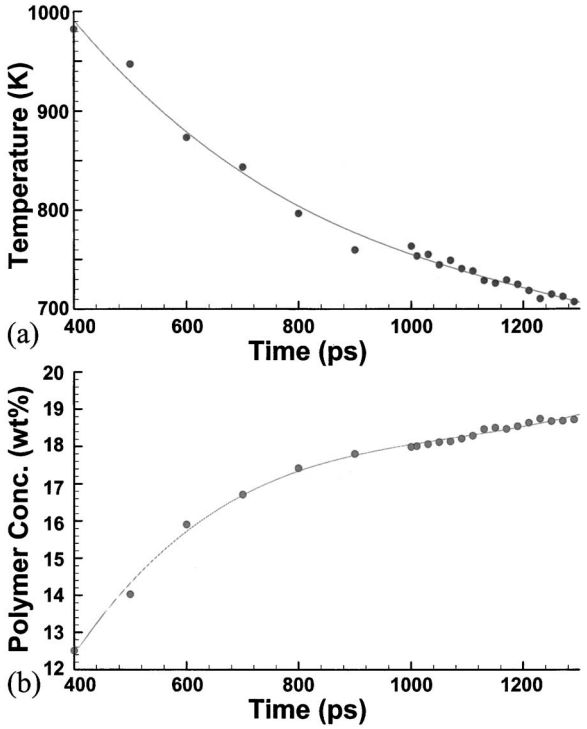


FIG. 5. Plot of the internal temperature (a) and polymer concentration (b) of the cluster shown in Fig. 4 as a function of time after ejection from the target. Both the polymer concentration and internal temperature of the cluster saturate as time progresses.

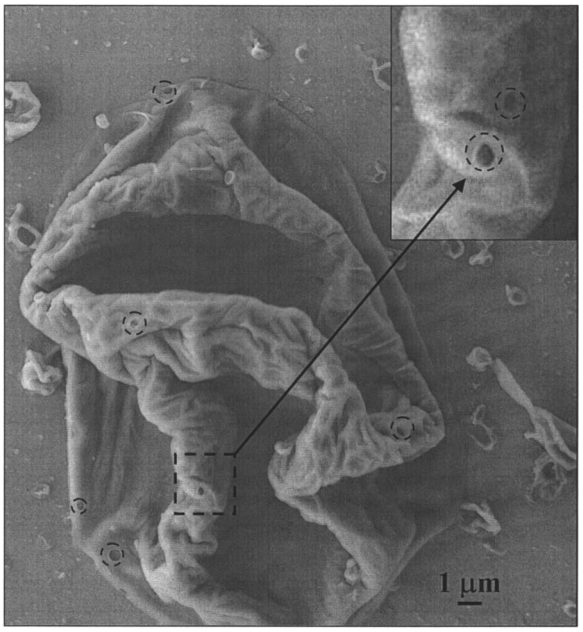


FIG. 6. SEM micrograph of a PMMA surface feature illustrating the characteristic deflated-balloonlike structure. Inset is a close-up image of the feature showing the presence of pores that may act as solvent-release sites.

experimentally. The changes in cluster shape are accompanied by the fast evaporation of toluene molecules and the decrease of the internal temperature of the cluster, as evident from Fig. 5. Within 900 ps following the detachment of the cluster, its internal temperature decreased by ≈300 K and the polymer concentration in the cluster increased by ≈6 wt %. As the simulation progressed, a continuous decrease in the rate of toluene evaporation from the cluster was observed. Likewise, a similar trend was observed for the internal temperature of the cluster. The saturation of both composition and temperature suggests that the cluster composition at 1.3 ns is similar to the composition of the cluster upon deposition onto the substrate. The polymer concentration in the cluster at this point in time is ≈18 wt %. Thus, the results of the simulations suggest that clusters reaching the surface can retain a significant amount of volatile matrix material.

Through a merger of experimental and computational findings, mechanisms underlying surface feature formation can be further elucidated. Based on the experimental and computational data gathered so far, the following scenario for surface feature and film formations is proposed. Laser ablation of the MAPLE target results in the ejection of large matrix-polymer clusters. The evaporation of toluene from these porous clusters of target material generates a polymer-rich membrane around each cluster. The membrane effectively slows down the diffusion of internal toluene molecules, inhibiting their escape from the interior of the cluster. As internal toluene molecules continue to evaporate, the polymer membrane "inflates." Eventually, escape passages are formed through the viscous polymer exterior, inducing a collapse of the polymer membrane as toluene vapor is exhausted from the cluster. It follows then that the wrinkled, deflated appearance of surface features, as shown in Fig. 6, is a result of subsequent particle collapse. The inset in Fig. 6 is a magnified image of what may be two of the final outlets for toluene vapor to escape.

Several depositions involving the addition of multiwalled nanotubes (MWNTs) to PMMA-toluene solutions were performed to observe the potential effects MWNTs have on the characteristic surface morphology observed during the deposition of PMMA. Although significant UV absorption by MWNTs can be expected to decrease the overall laser penetration depth of the target,[18] the experimental conditions are likely to remain conducive to matrix-polymer cluster formation. Figure 7 is a SEM micrograph of surface features observed on a PMMA film infused with MWNTs. The film was created using a polymer concentration of 3 wt %, a MWNT concentration of 1 wt %, and a laser fluence of 0.40 J/cm$^2$. Like the surface features resulting from MAPLE of strictly PMMA in toluene, the surface features in the image also possess deflated structures, implying that even when MWNTs are added to the target solution, clusters of material continue to be ablated from the target and subsequently deposited onto the substrate in the same manner previously described, as expected. The implications of this finding are encouraging, as a MAPLE process developed to reduce the surface morphology of pure PMMA films could potentially be extended to achieve significant improvements in PMMA nanocomposite thin film morphologies.

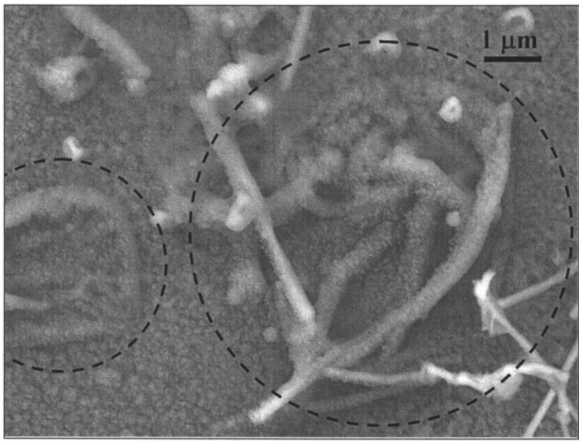


FIG. 7. SEM micrograph of surface features observed on a PMMA/MWNT film using a PMMA concentration of 3 wt %, a MWNT concentration of 1 wt %, and a laser fluence of 0.40 J/cm$^2$. The underlying morphology of the PMMA/MWNT film appears to be dominated by surface features similar to those associated with previous MAPLE depositions of pure PMMA, shown in Figs. 1 and 2.

## IV. SUMMARY

Thin films of PMMA were successfully deposited onto Si substrates via MAPLE using toluene as the sacrificial matrix solvent. The surface morphology of the films was characterized as a function of both laser fluence and polymer loading in the target. Experiments and molecular dynamics simulations were run in parallel to examine the mechanisms responsible for material ejection and film formation. The morphology of deposited films suggests that clusters of target material containing both toluene and PMMA were ejected from the target and subsequently deposited onto the substrate. In general, increases in laser fluence and polymer concentration resulted in an increase in the size and number density of surface features. Composite PMMA/MWNT films deposited via MAPLE showed surface features similar to those found in pure PMMA MAPLE films. Future work will further investigate surface feature formation using controlled-temperature experiments, time-gated imaging, and computer modeling.

## ACKNOWLEDGMENTS

Financial support for this work was provided by the National Science Foundation through Grant No. DMII-0422632 under Dr. Kevin Lyons.

[1]R. A. McGill and D. B. Chrisey, U.S. Patent No. 6,025,036 (15 February 2000).
[2]D. M. Bubb, P. K. Wu, J. S. Horwitz, J. H. Callahan, M. Galicia, A. Vertes, R. A. McGill, E. J. Houser, B. R. Ringeisen, and D. B. Chrisey, J. Appl. Phys. **91**, 2055 (2002).
[3]D. M. Bubb, M. R. Papantonakis, J. S. Horwitz, R. F. Haglund, Jr., B. Toftmann, R. A. McGill, and D. B. Chrisey, Chem. Phys. Lett. **352**, 135 (2002).
[4]A. L. Mercado, C. E. Allmond, J. G. Hoekstra, and J. M. Fitz-Gerald, Appl. Phys. A: Mater. Sci. Process. **81**, 591 (2005).
[5]P. K. Wu, J. M. Fitz-Gerald, A. Pique, D. B. Chrisey, and R. A. McGill, in *Laser-Solid Interactions for Materials Processing*, MRS Symposia Proceedings No. 617, edited by D. Kumar, D. P. Norton, C. B. Lee, K. Ebihara, and X. Xi (Materials Research Society, Pittsburg, 2000), p. J2.3.1.
[6]M. C. Paiva, B. Zhou, K. A. S. Fernando, Y. Lin, J. M. Kennedy, and Y. P. Sun, Carbon **42**, 2849 (2004).
[7]W. Zheng and S. C. Wong, Compos. Sci. Technol. **63**, 225 (2003).
[8]J. Jordan, K. I. Jacob, R. Tannenbaum, M. A. Sharaf, and I. Jasiuk, Mater. Sci. Eng., A **393**, 1 (2005).
[9]D. M. Delozier, K. A. Watson, J. G. Smith, and J. W. Connell, Compos. Sci. Technol. **65**, 749 (2005).
[10]L. J. Lee, C. Zeng, X. Cao, X. Han, J. Shen, and G. Xu, Compos. Sci. Technol. **65**, 2344 (2005).
[11]T. Kashiwagi, F. Du, K. I. Winey, K. M. Groth, J. R. Shields, S. P. Bellayer, H. Kim, and J. F. Douglas, Polymer **46**, 471 (2005).
[12]Y. Liu, K. Gall, M. L. Dunn, and P. McCluskey, Mech. Mater. **36**, 929 (2004).
[13]L. V. Zhigilei, Y. G. Yingling, T. E. Itina, T. A. Schoolcraft, and B. J. Garrison, Int. J. Mass. Spectrom. **226**, 85 (2003).
[14]L. V. Zhigilei, E. Leveugle, B. J. Garrison, Y. G. Yingling, and M. I. Zeifman, Chem. Rev. (Washington, D.C.) **103**, 321 (2003).
[15]E. A. Colbourn, *Computer Simulations of Polymers*, 1st ed. (Longman Scientific and Technical, Harlow, Essex, 1994).
[16]R. Kelly and A. Miotello, J. Appl. Phys. **87**, 3177 (2000).
[17]L. V. Zhigilei, Appl. Phys. A: Mater. Sci. Process. **76**, 339 (2003).
[18]P. D. Kichambare, L. C. Chen, C. T. Wang, K. J. Ma, C. T. Wu, and K. H. Chen, Mater. Chem. Phys. **72**, 218 (2001).